Supplement of Earth Surf. Dynam., 9, 463–485, 2021
https://doi.org/10.5194/esurf-9-463-2021-supplement

Supplement of

Implications of the ongoing rock uplift in NW Himalayan interiors

Saptarshi Dey et al.

Correspondence to: Saptarshi Dey (saptarshi.dey@iitgn.ac.in)

Supplement section S1

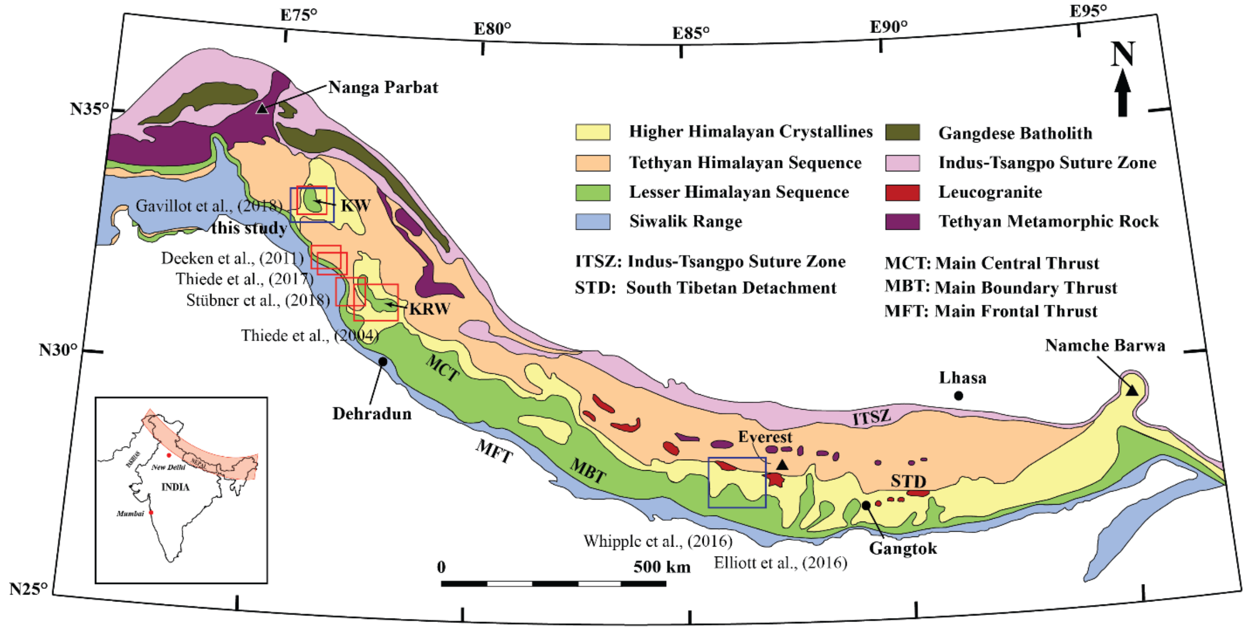

Fig. S1: A generalized geological map of the Himalayan orogen (modified after Yin and Harrison, 2000; DiPietro and Pogue, 2004) showing the spatial distribution of major morphotectonic sectors. Locations of crucial low-T thermochronology studies in the NW Himalaya are shown (Thiede et al., 2004; Deeken et al., 2011; Thiede et al., 2017; Stuebner et al., 2018; Gavillot et al., 2018).

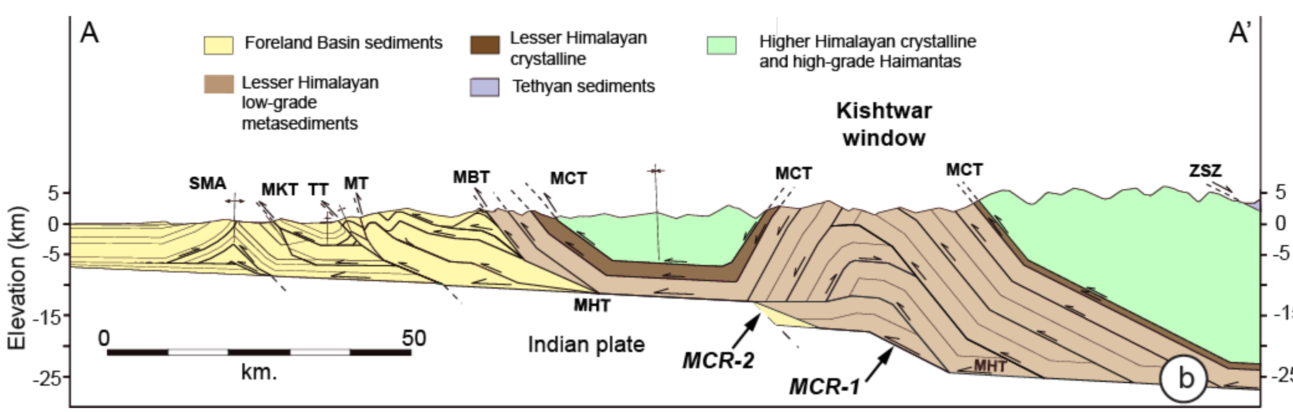

Fig. S2: Balanced cross-section across the Jammu-Kishtwar sector of the NW Himalaya (modified after Gavillot et al., 2018), showing model-predicted structural variations of the Himalayan orogenic wedge. Important to note the two small mid-crustal ramps (MCR-1 and MCR-2) emerging from the MHT, lying beneath the Lesser Himalayan duplex. They propose a higher exhumation rate of the LH duplex (3.2-3.6 mm/a) since Quaternary.

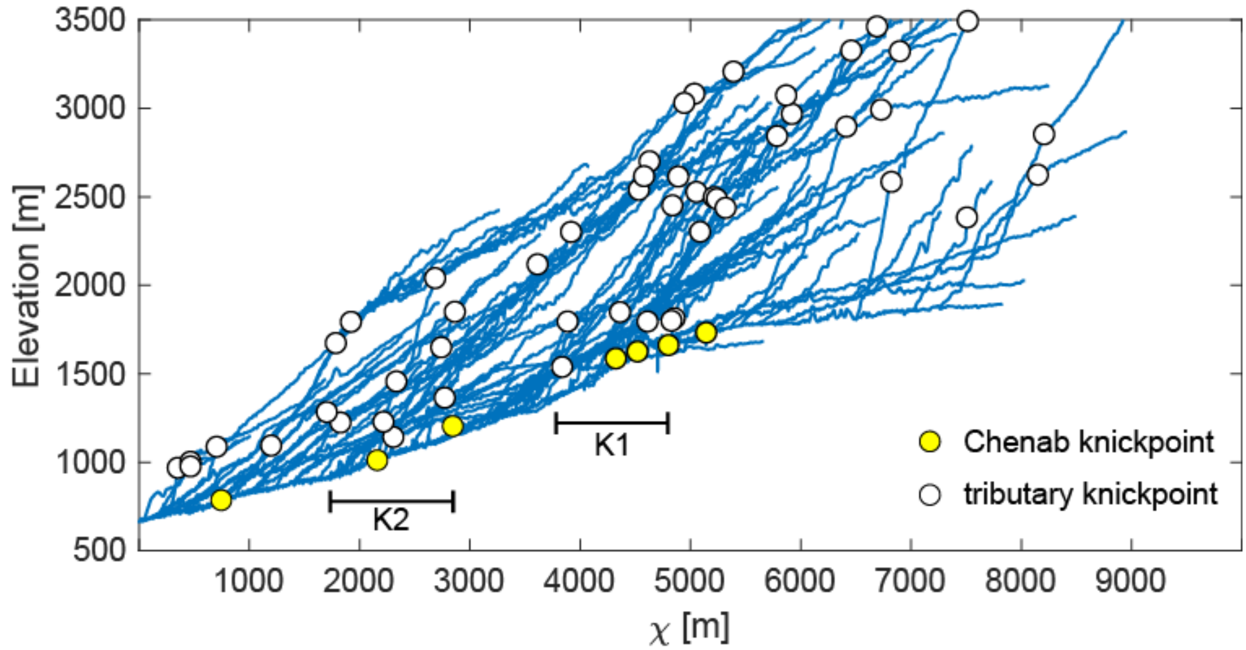

Fig.S3: Chi vs. elevation plot of the Chenab drainage system showing major knickpoints.

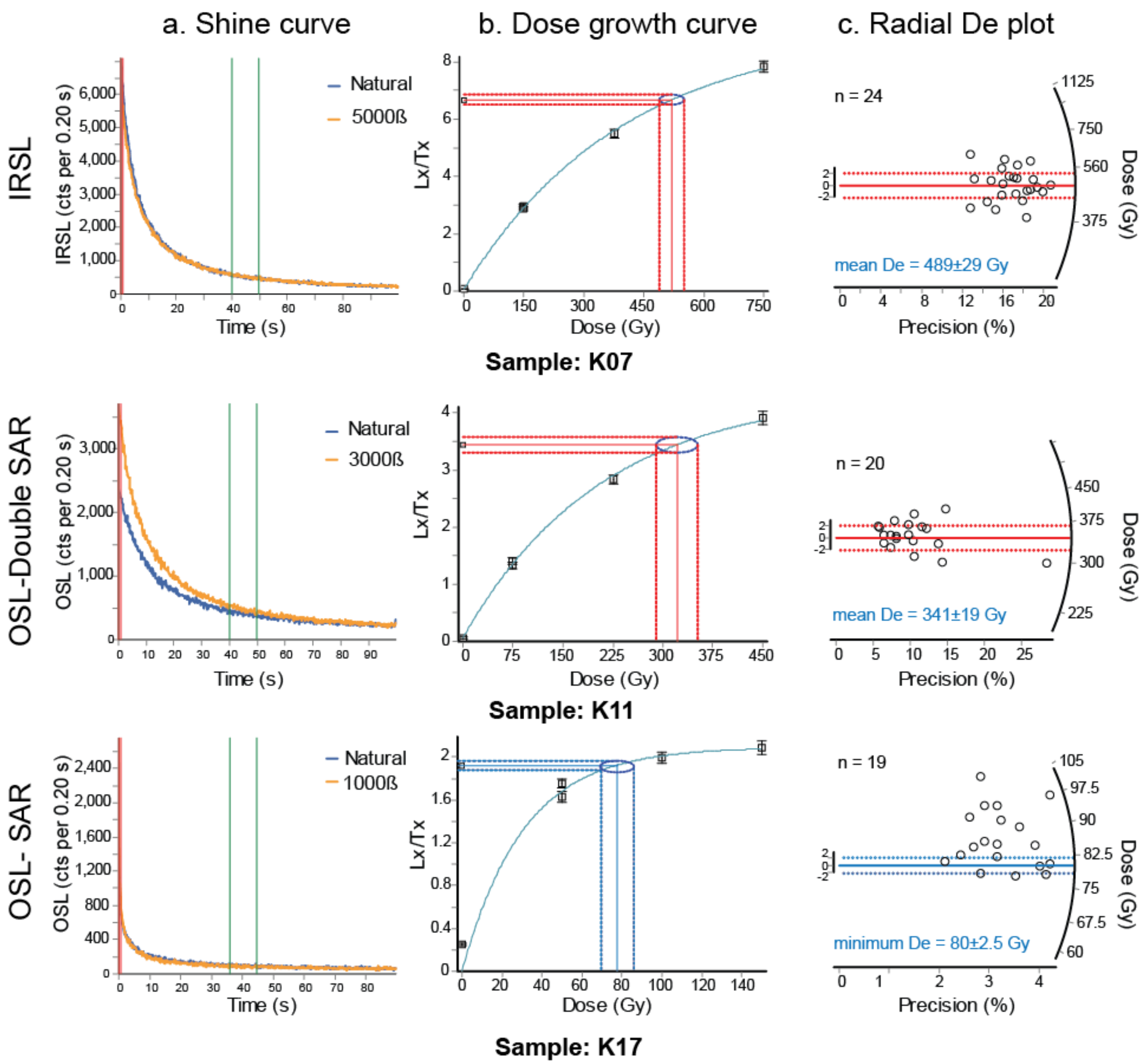

Figure S4: (a) Shine curve, (b) dose growth curve, and (c) radial De estimation plot for the three different luminescence dating protocols used in this study.

Supplementary Table S1:

Site	latitude	longitude	rock type	Dist. (km)	R1	R2	R3	R4	R5	R6	R7	R8	R9	R10	R11	R12	Mean_R	stdev_R	lithology_mean R	lithology_R_sigma
1	33.1842	75.3047	LH MS	1	39.9	39.3	40.6	40.3	42.3	41.5	40	40.7	40.9				40.6	0.8	41.1	1.9
2	33.1664	75.3123	LH MS	2.3	40	40.2	40	39	39.2	40.3	39.2	40.9	41	41.2			40.0	0.7		
3	33.1604	75.3253	LH MS	4.2	39.8	39	39.5	40.2	39.1	40.2	40.4	38.9	39.2	39.4	39.6		39.6	0.5		
4	33.1497	75.3485	LH MS	6.5	41.3	41.5	40.5	43.8	43.4	38.9	39.2	41.8	42				41.4	1.6		
5	33.139	75.3671	LH MS	10.8	40.1	37.8	37.7	37.2	39	38.8	39.2	39	39.1	38.5			38.7	0.9		
6	33.1343	75.3797	LH MS	13.4	42	40.6	40.2	39.6	39.9	42.2	41.4	41.8	41.1	41.6			41.0	0.9		
7	33.1317	75.4039	LH MS	17.5	43.1	43.5	40.2	40.9	43.9	45	44.1	43.4	42.9				43.0	1.4		
8	33.1266	75.417	LH MS	19	44	43.8	45.2	43.7	42	40.2	40.8	43.3	44.4	44.6			43.0	1.6		
9	33.1287	75.4281	LH MS	22.1	43.1	43.2	44.5	44	44.7	40.3	41.6	42.3	43	42.9			43.0	1.3		
10	33.134	75.4411	Haimanta	24.6	45	44.3	44.4	41.5	40.8	40	43.4	43.2	42	40.1	40.5	44	42.4	1.7	44.5	2.2
11	33.1306	75.4547	Haimanta	26.2	47.2	47	45.5	48.2	47.9	46.6	47	47.1					47.1	0.8		
12	33.1373	75.4619	Haimanta	28.8	47.7	48	49.1	48.2	49	46.2	46.6	46.7	47.3	47.8			47.7	0.9		
13	33.1372	75.4747	Haimanta	32.1	43.4	42	42.9	44.1	42	43.1	43.6	43.3	43.2	43	41		42.9	0.8		
14	33.1352	75.4843	Haimanta	33.2	43.5	43.7	44	43.3	43.3	44.4	44.5	44	42.8	43.9			43.7	0.5		
15	33.1398	75.4995	Haimanta	34	44.1	44.5	45	44.5	44.3	44.8	43.6	43.8	44.4				44.3	0.4		
16	33.1404	75.5219	HHCS	36.9	36.6	36.9	35.3	35.9	36.6	37	37.3	36.8	38	37.1	35.6	36	36.6	0.7	38.9	2.4
17	33.1316	75.5482	HHCS	38.1	41.1	41.2	42.6	40	40.4	41.3	42.8	38	42.3	38.7	40.9		40.8	1.4		
18	33.1362	75.5618	HHCS	42	40.8	40.3	42.3	39	39.4	40.9	42.2	42	39.6	40	40.1		40.6	1.1		

19	33.1361	75.5857	HHCS	43.6	38.8	39	39.2	39.9	37.2	37.9	39.9	38.3	38	37.9	38		38.6	0.8		
20	33.132	75.6025	HHCS	45	35.9	36	36.2	35.8	37.2	36.9	38	36.8	39	37.5	37.2	38.2	37.1	1.0		
21	33.1211	75.6232	HHCS	47.5	39	39.8	39	38.9	37.1	40.4	40.1	37.3	38	36.9	40.3		38.8	1.2		
22	33.1217	75.6399	HHCS	48.2	39.5	38.9	39	39.8	40.2	37.1	40.4	38.4	37.9	37	38.1	37.5	38.7	1.1		
23	33.1304	75.656	HHCS	48.7	42.1	40	39.8	37.5	37.8	37.8	38.6	39	38.4	37.3	39.9		38.9	1.4		
24	33.1498	75.6753	HHCS	49.3	40.4	40.2	41.1	41.3	45	40.7	38.4	40.2	43.7	44	37.6		41.1	2.2		
25	33.1471	75.6649	HHCS	50	37.7	38	38.9	37.8	39.2	39.1	38.8	39	39.9	37.7			38.6	0.7		
26	33.1489	75.7136	HHCS	51.1	40.7	40.7	40	38.8	39.1	39.1	39.7	39.2	40	37.8	37.4	37.3	39.2	1.1		
27	33.1527	75.7408	HHCS	51.4	40.5	40.3	39.8	36.9	37	42.3	40.3	40	37.2	38.7	39		39.3	1.6		
28	33.1352	75.759	HHCS	53	42.4	42.2	40.6	45.7	40.2	39.2	39.9	42.1	43	43.2	41.5		41.8	1.7		
29	33.149	75.8031	HHCS	55.2	39.6	39.9	39.2	39	38.3	40.6	41.1	39.9	38.6	39.8	40		39.6	0.8		
30	33.1611	75.8064	HHCS	57.5	38	36.8	37	37.2	38.9	36.6	36.4	37.2	37	38.2	38.1		37.4	0.7		
31	33.1832	75.8146	HHCS	60.3	37.6	36.9	37	35.8	36	37.2	38.1	36.7	35.4	36.7			36.7	0.8		
32	33.1913	75.8107	HHCS	63.4	36	34.4	35.8	32.3	35	30.1	28.9	33.1	32.2	31.5	35.3		33.1	2.3		
33	33.2068	75.8036	HHCS	67.9	39.3	39.2	37.9	37.3	40	38.4	38.6	39.8	40.1	39.6	39.9		39.1	0.9		
34	33.2256	75.8014	HHCS	72.2	39.9	40.6	40.3	39.8	39.8	41.3	41.5	40.8	41	41.1	41.2		40.7	0.6		
35	33.2304	75.7918	HHCS	73.6	44.7	40.1	40.2	40.2	41.1	41.3	40.4	43.2	42.6	40.4	40.9		41.4	1.4		
36	33.2405	75.7895	HH mg	74.5	37.7	34.2	30.4	30.6	32.2	30.9	31.1	30	34.1	30.4			32.2	2.3	48.9	6.7
37	33.2493	75.7824	HH mg	75.4	44	44.9	43.9	43.8	44.2	45.7	45.2	43.1	43	42.6	43	44	43.9	1.0		
38	33.2614	75.7753	HH mg	76.8	43.7	44	45.3	45.2	44.8	44.3	44.9	45	45.5	44.8	43.1	45.2	44.6	0.7		
39	33.2674	75.7746	HH mg	77.3	45.5	45.3	46.2	45.2	44.9	45.3	48	46.2	46.3	46.8			46.0	0.9		
40	33.2728	75.7698	HH mg	78.8	45.3	45.4	47	46.7	45.9	45.3	46	45.6	45.1	45	46		45.8	0.6		

41	33.2829	75.7699	HH mg	79.2	48	46.6	45.9	46	45.7	46	45.8	46.3	45.9	46.3	46	46.2	0.6		
42	33.2897	75.7644	HH mg	80.1	45.9	47.8	48	49.2	49.4	48.5	49.5	47.3	48.9	49.5	49.2	48.5	1.1		
43	33.2918	75.754	HH mg	80.6	46.9	46.5	47.2	47.2	46.9	47.4	47.1	46	46.2	45.9	47.1	46.8	0.5		
44	33.3316	75.7271	HH mg	82	47	47.2	46.6	46.9	46.2	47.4	46.5	47.2	46	45.9	46.2	46.6	0.5		
45	33.3443	75.7296	HH mg	92.4	47	47.2	48.2	48.1	47.7	47	48.2	46.9	47.3	48		47.6	0.5		
46	33.3578	75.7225	HH mg	93	50.1	50	48.8	48.8	46.4	48	47.2	46.9	47.3	48.2		48.2	1.2		
47	33.3383	75.7256	HH mg	94.8	58.3	56.9	55	57.2	52.6	55.6	55.9	56	56.3	57.2	55.2	56.0	1.4		
48	33.3497	75.7329	HH mg	100.1	60.5	58.9	60.1	59.2	59	60	58.3	58.8	58.9	59	59.1	59.3	0.6		
49	33.3227	75.743	HH mg	102.5	62.9	60.7	61	61.5	60.3	60.5	59.9	60.2	60.3	59.9	62	60.8	0.9		
50	33.3577	75.7345	HH mg	104.2	50.6	54.7	53.9	53.8	54	50.8	52	53.9	54	52.5	53.2	53.0	1.3		
51	33.3603	75.749	HH mg	105.8	56.2	56	55.9	54.3	51.9	56.8	57	55.5	56	53.8	55.7	55.4	1.4		
52	33.3737	75.7539	LH schist	108.2	37.9	36.9	37.8	39.3	38.2	38	38.2	37.7	39.2	38		38.1	0.7		
53	33.377	75.7759	LH qt	110.2	54.9	53.4	54	54.4	52.5	53.2	55	54.7	54.1	55	54.2	54.1	0.8	51.6	4.8
54	33.3708	75.7879	LH qt	112.1	51	51.9	53.3	54.2	54.5	52.9	52.8	52.5	53.8	53		53.0	1.0		
55	33.3586	75.8062	LH qt	114.7	49.9	50.3	50.5	49.5	51	51	50.2	49.2	50.3	49.8		50.2	0.6		
56	33.3578	75.8286	LH qt	115.8	50.5	52.1	50.4	50.9	48.4	47.9	52	51.1	50.5	50.9		50.5	1.3		
57	33.353	75.8478	LH qt	117.6	48.7	48.9	50	49.4	47.3	47	47.1	48.4	48.2	46.5		48.2	1.1		
58	33.3535	75.8654	LH qt	121	50.5	54.1	55	53.2	55.9	52.1	54.8	54.1	53.1	55.4		53.8	1.6		
59	33.3412	75.8917	LH qt	123.2	57.2	53.1	53.2	56	55.7	52.7	57.1	54.3	56.6	56.3		55.2	1.6		
60	33.3438	75.9054	LH qt	126.5	57.8	56.9	57.1	53.3	59	55	57.2	58.8	57.5			57.0	1.7		
61	33.3437	75.9238	LH qt	130.9	52.9	53	55.3	54.6	55	52.4	57.7	53.3	55.2	54.3		54.4	1.5		
62	33.3349	75.9373	LH qt	132.3	40.3	45.2	37.3	37	38.3	44	39.2	41	41.1	36.9		40.0	2.7		

63	33.3381	75.9574	LH gr	133.8	53.6	53	54.5	54.1	52.8	52.5	53.3	53.9	50.8	52.9			53.1	1.0	55.4	3.0
64	33.3272	75.9669	LH gr	135	49.9	48.8	49.1	53	50.7	48.3	50.8	53.5	50.6	52.4	53.1		50.9	1.8		
65	33.3183	75.9932	LH gr	138.4	55.8	55.7	57.1	57.3	57	56.7	56.4	55.9	56	56.9	57		56.5	0.6		
66	33.3228	76.0164	LH gr	139.6	56.1	56.8	57	57.4	57.3	58.7	58	58.1	57.9	58.5	58.7	58	57.7	0.8		
67	33.3293	76.0406	LH gr	140	58	58.1	58.9	60.1	57.8	57.9	58	58.5	58.2	57.9			58.3	0.7		
68	33.3164	76.0556	LH qt	141.6	62.6	61.1	60.7	61.1	60.5	60.2	59.7	60.5	61.2	60.7			60.8	0.7		
69	33.3123	76.07	LH qt	143.6	56.6	56.9	57	56.4	56.6	57.5	55.2	56.8	56.7	58			56.8	0.7		
70	33.3055	76.0779	LH gr	147.8	59	59.3	57.8	58.8	60.1	59.2	58.9	59.7	59	57.3			58.9	0.8	58.1	1.6
71	33.2967	76.0874	LH gr	148.4	59.9	59.3	59.8	57.8	58	58.6	59.9	60.5	59.9	59.8			59.4	0.9		
72	33.2925	76.1009	LH gr	152.5	60.3	60.2	61.2	60	58.9	59.2	59.2	59.9	60.1	59.1			59.8	0.7		
73	33.2783	76.1112	LH gr	154.6	58.6	56.9	56.8	57	57.5	58.2	56	56.6	55.9	56			57.0	0.9		
74	33.2628	76.119	LH gr	157.6	59	56.7	55	55.4	55.9	57.2	57.5	57	58.3	55.5			56.8	1.2		
75	33.2586	76.1389	LH gr	158.8	58.2	57.7	57.7	55.9	56	58.2	58.4	55	55.2				56.9	1.3		

Table S1: Details of site-specific R-values collected using rock-rebound hammer. [Abbreviations: LH MS – Lesser Himalayan Metasediments, LH gr – Lesser Himalayan granite, LH qt – Lesser Himalayan quartzite, HHCS – Higher Himalayan crystalline sequence, HH mg – Higher Himalayan migmatites).

Supplement S2

Luminescence sample preparation

The samples for luminescence dating were collected in galvanized iron pipes. The pipes were opened in subdued red light (wavelength ~650 nm). The outer ~3 cm of sediment from both the ends of the pipe were removed to omit possibility of exposure of sample to daylight during collection. The removed portion was used for moisture content estimation and determination of Uranium (U), Thorium (Th) and Potassium (K) concentrations. The interior unexposed portion of sample was further processed to obtain quartz and feldspar using standard procedures (e.g. Aitken, 1998). The portion was treated with sufficient quantity of 1N HCl and 30% H_2O_2 to remove carbonates and organic materials respectively. The sediments were then oven dried at 45°C and sieved to obtain a size fraction of 90-150 µm. The quartz and feldspar were separated using Frantz isodynamic separator at a magnetic field of ~10,000 gauss and collected separately. Obtained quartz grains were etched with 40% HF for 80 minutes to remove alpha irradiated outer layer (~10 µm) followed by 37% HCl treatment for 20 minutes to dissolve fluorides formed during previous step. The isodynamic separation procedure was repeated to remove any broken feldspar grain. However, even after repeating the last step for 2 times, we were unable to completely eliminate the feldspar contamination from the samples.

Samples K02 and K11 procured from the fine-grain layers of ~1-1.5m thickness, trapped within coarse, angular and poorly-sorted thick layers of clasts (identified as hillslope debris) were used for OSL (Optically stimulated luminescence) dating using Double SAR (Single Aliquot Regenerative) protocol (IRSL wash before OSL measurement) for equivalent dose estimation (Roberts, 2007). The test doses were set for 75 Gy, 225 Gy and 450 Gy, respectively (Fig.5). The aliquots were considered for ED estimation only if: (i) recycling ratio was within 1±0.1, (ii) ED error was less than 20%, (iii) test dose error was less than 10%, and (iv) recuperation was below 5% of the natural. Samples K01 and K06, taken from fluvial sand layer lying just above the Higher Himalayan bedrock strath in the east of the town of Doda were also treated for OSL double-SAR method.

OSL dating for the three samples procured from the fluvio-glacial sediments showed saturation; therefore, we tried for IRSL (Infra-red stimulated luminescence) dating of feldspar for those three samples (K07-K09) using standard post infrared (pIR-IR) protocol (Biswas et al., 2013; Buylaert et al., 2013), in which, the preheat temperature was 320°C for 60s. The samples were first stimulated at 50°C with IR diodes for 100s followed by IR stimulation at 290°C and a violet-blue luminescence emission (395 ± 50 nm) was detected by PMT through the combination of optical filters, Corning 7-59 (4 mm) and BG-39 (2 mm). However, the samples showed significant saturation possibly due to improper bleaching of Post-IR IRSL signal, however the IRSL signal is not saturated suggesting it to be better bleached. We encountered significant IRSL signal while testing the luminescence of hand-picked individual quartz grains suggesting a presence of feldspar inclusion within the quartz. We tried leaching with 40% HF for three times, which exhausted most of the separated quartz sample. Hence, we had to proceed with standard IR protocol (Preusser, F., 2003) using K-feldspar. The initial test dose for the samples was set for 150 Gy and the rest of the runs were set for 375 Gy and 750 Gy, respectively (Fig.5). Fading correction tests were done for two samples SD_K07 and SD_K09 and the fading correction factors have been calculated using conventional methods after Huntley and Lamothe, (2001). The over-dispersion values are less than 30% (Table 1) and hence, Central Age Model (CAM) has been used for estimation of equivalent dose (De) (Bailey and Arnold, 2006) instead of De estimation as prescribed by Chauhan and Singhvi, (2011), useful for samples having higher over dispersion.